Zirconium under pressure: structural anomalies and phase transitions

2003 J. Phys.: Condens. Matter 15 5009

(http://iopscience.iop.org/0953-8984/15/29/312)

INSTITUTE OF PHYSICS PUBLISHING JOURNAL OF PHYSICS: CONDENSED MATTER

J. Phys.: Condens. Matter **15** (2003) 5009–5016 PII: S0953-8984(03)62906-1

Zirconium under pressure: structural anomalies and phase transitions

F Jona and P M Marcus

Department of Materials Science and Engineering, State University of New York, Stony Brook, NY 11794-2275, USA

E-mail: fjona@ms.cc.sunysb.edu

Received 30 April 2003
Published 11 July 2003
Online at stacks.iop.org/JPhysCM/15/5009

Abstract

The full-potential linearized augmented plane-wave method within the local-density approximation is used to investigate the effect of hydrostatic pressure on the structure of zirconium metal. Three phases are considered: hexagonal close-packed (hcp); body-centred cubic (bcc); and ω. For each of them the Gibbs free energy $G = E + pV$ is calculated as a function of hydrostatic pressure. The three free energies as functions of pressure show three phase transitions at 0 K: hcp to bcc at 23 kbar; ω to bcc at 50 kbar; and ω to hcp at 87 kbar. The ground state at 0 K is ω up to 50 kbar and bcc above 50 kbar. Anomalies in the hcp structure and elastic constants at 0 K are found from 0 to 50 kbar.

1. Introduction

Zirconium metal has been the object of several experimental and theoretical studies, both at ambient pressure ($p = 0$) and at higher hydrostatic pressures ($p \neq 0$) [1–7]. The experiments show that, at $p = 0$ and room temperature, Zr has hexagonal close-packed (hcp) structure [8], but becomes body-centred cubic (bcc) at temperatures higher than 860 °C [9].

Under increasing pressure at room temperature, the hcp phase transforms into a hexagonal structure called the ω phase which, in turn, at higher pressures transforms into the bcc phase [6, 7]. The ω phase is *not* close-packed (space group number 191, $P6/mmm$), it has three atoms per unit cell, and is found in a number of elements and alloys (Ti, Hf, CdI_2, AlB_2, MgB_2, Be_2Hf, etc) [10]. In Zr the ω phase can be retained in a metastable state at ambient conditions [9]. The transition from hcp to ω has been reported in the literature to occur at various pressures in the range between about 20 and 60 kbar [11–14] at 20 °C and at 9.2 kbar at −200 °C [9]. However, it is now believed to occur at 22 kbar [6] at room temperature. The reverse transition, ω to hcp, was stated to happen at ambient pressure at 200 °C [9]. The transition pressure between ω and bcc is reportedly 300–350 kbar [6, 7]. The lattice parameters of hcp, bcc and ω Zr at $p = 0$ are summarized in table 1.

Table 1. The lattice parameters of Zr structures. Abbreviations: hcp = hexagonal-close-packed; bcc = body-centred cubic. The ω data refer to the quenched structure released from high-pressure; lattice lengths are in ångström [8].

Structure	Temp. (°C)	a	c	c/a
hcp	25	3.2312	5.1477	1.5931
bcc	862	3.6090		
ω		5.0336	3.109	0.617

Theoretical studies of Zr under pressure have been performed with either the full-potential linear muffin-tin orbital (FP-LMTO) method [1, 3, 5] or the full-potential linearized augmented plane-wave (FP-LAPW) procedure [2, 4], mostly within the local-density approximation (LDA) but sometimes also with the generalized-gradient approximation (GGA). Common to all these studies is the calculation of energy versus volume [$E(V)$] curves; in some cases the axial ratio c/a is kept constant. These curves are used to find the value of the volume at which the curves of two structures cross, in order to determine a phase transition. The transition volume is then converted to transition pressure by means of the equation of state, which requires the evaluation of the derivative $\mathrm{d}E/\mathrm{d}V$. Two criticisms may be raised against these procedures. One is that the assumption of constant c/a is an approximation which may cause significant errors in the determination of the energy, and the subsequent derivative of the energy, in calculating the pressure. The other is that, at finite pressures, phase transitions are found from the crossings of $G(p)$ curves, not $E(V)$ curves. Nevertheless, all studies find the *sequence* of structures with increasing pressure to be hcp $\rightarrow \omega \rightarrow$ bcc, in agreement with room-temperature experiments. Whenever *both* the LDA and the GGA were used, the LDA transition pressures were found to be considerably lower than the GGAs, but the GGA values agree better with the experimental results.

In the work presented here we attempted to avoid the two criticisms mentioned above by allowing both the volume and the axial ratio to vary, and by minimizing the free energy at each pressure rather than the energy at each volume. We used a first-principles total-energy method and we opted for the LDA for the following reason. Our previous work on the epitaxial Bain path of tetragonal Zr at $p = 0$ [15] found that the bcc phase is metastable when calculated with the LDA but is unstable when calculated with the GGA. Since the bcc phase of Zr is known to be stable at $p = 0$ and higher temperatures, as well as at finite pressures, the LDA appeared to be a better choice. We thus calculated the free energies of the three phases (hcp, ω and bcc) at equilibrium as functions of pressure, and determined the phase transition pressure from the crossing points of $G(p)$ curves. We found that the elastic constants of the hcp phase exhibit marked anomalies at the transition pressures, but we did not obtain the structure sequence found experimentally with increasing pressure at room temperature. We present details of the calculations in section 2, the results in section 3, and the discussion in section 4.

2. Details of the calculations

We used the WIEN97 computer program, which is designed to apply the FP-LAPW method to calculations of total energies for a variety of crystal structures and space groups [16]. As mentioned in the introduction, we opted for the nonrelativistic LDA approximation to describe exchange and correlation effects.

For each of the three structures considered (hcp, ω and bcc) we aimed at high precision in the determination of the total energy by using: a large plane-wave cutoff of $RK_{\max} = 9$; a magnitude of the largest vector in the charge density Fourier expansion of $G_{\max} = 14$ bohr^{-1}

and a criterion of 1×10^{-6} Ryd for energy convergence. For both the hcp and the bcc structures we chose 20 000 k-points in the full Brillouin zone (BZ), corresponding to 1026 and 1470 k-points, respectively, in the irreducible wedge of the BZ and resulting in 1350 and 475 plane waves, respectively. For the ω structure the parameters were 3000 k-points in the full BZ, 190 k-points in the irreducible BZ, and 2000 plane waves. The muffin-tin radius of Zr was kept at 2.0 bohr for all calculations.

The aim of the calculations, for all three structures considered, was to determine the equilibrium structure as a function of pressure p, and in the process determine the free-energy function $G(p)$ at equilibrium at each pressure p, the lattice parameters $a(p)$ and $c(p)$, and the volume/atom $V(p)$. The procedures were described in detail in our study of magnesium under pressure [17] and are only briefly summarized here. For a chosen value of the pressure p:

(1) select a value of $a = a_1$;
(2) for several values of c calculate the total energy E;
(3) find the value of $c = c_1$ and $E = E_1$ at which the slope of the energy function $E(c)$ is $(\partial E/\partial c)_a = -(a^2 \sin\gamma/2)\,p$, with $\gamma = 60°$ for hcp and ω and $\gamma = 90°$ for bcc (this value is the one at which the stress in the c-direction equals $-p$);
(4) calculate the volume $V_1 = \frac{1}{2}a_1^2 c_1 \sin\gamma$;
(5) evaluate $G_1 = E_1 + pV_1$;
(6) repeat the procedure from (1) through (5), for the same chosen value of p, but for a number of different values of a such as to bracket the minimum of G;
(7) find this minimum by fitting a cubic polynomial (or a parabola) to the $G(a)$ values, thereby determining the values of the parameters a, c, c/a and V for the chosen pressure p.

The next step is to choose another value of the pressure and repeat the procedure from (1) through (7), then choose another p etc. It should be clear that, in each step, we determine the minimum of the free energy and, after several steps, we are in a position to plot $G(p)$, $a(p)$, $c(p)$ and $V(p)$.

For the hcp structure we also determined the pressure dependence of the bulk modulus B and of the ratio between linear compressibilities k_c and k_a along the c and a directions, respectively, expecting to find anomalies in the vicinity of phase transitions. These quantities are found from second derivatives of the G function, as described in [18]. A 'constrained' bulk modulus $B_{(c/a)}$ is found by keeping the axial ratio c/a constant:

$$B_{(c/a)} = \frac{2}{9}\left(c_{11} + c_{12} + 2c_{13} + \frac{c_{33}}{2}\right). \tag{1}$$

But, allowing for a change in c/a when the volume changes so as to minimize G, the full bulk modulus is

$$B = \frac{c_{33}(c_{11} + c_{12}) - 2c_{13}^2}{c_{11} + c_{12} + 2c_{33} - 4c_{13}}. \tag{2}$$

The ratio k_c/k_a of linear compressibilities in the c and a directions is given by [19]

$$\frac{k_c}{k_a} = \frac{c_{11} + c_{12} - 2c_{13}}{c_{33} - c_{13}}. \tag{3}$$

The elastic constants needed to evaluate these quantities are calculated from second strain-derivatives of G at the minimum. The procedures for the calculation of elastic constants are described in previous papers and summarized in [17].

3. Results

Figure 1 depicts the free energy G as a function of pressure p for the three phases of Zr studied here (hcp, bcc and ω). The top panel shows that the three G curves are very close and almost parallel to one another, so that the relative magnitudes and intersections are difficult to see. For this reason we have plotted portions of the $G(p)$ plane in the lower panels with magnified scales. We note that:

(1) at $p = 0$ the lowest-energy phase is the ω phase, the next higher is the hcp phase, and the highest is the bcc phase;
(2) at approximately 20 kbar (second panel from the top) the free energies of the bcc and hcp phases cross, as the bcc phase becomes lower in energy at higher pressures, but the energy of the ω phase is still lower than the other two;
(3) at about 50 kbar (third panel from the top) the free energies of the bcc and the ω phases cross, as the bcc phase becomes lower at higher pressures;
(4) at about 87 kbar (bottom panel) the ω phase crosses the hcp phase, although the bcc phase is lower in free energy than both the hcp phase and the ω phase.

The pressure dependence of the lattice parameters is depicted in figure 2, where we see that both the a and the c parameters of the hcp structure exhibit small anomalies in the range between 0 and 50 kbar. The parameters of the bcc and ω phases do not show anomalies, except for a slight change in slope of those of the ω phase at about 50 kbar. This behaviour is reflected in the pressure dependence of the axial ratio c/a, depicted in figure 3.

Figure 4 shows the volume versus pressure curves. At $p = 0$ the bcc phase has the smallest volume, followed by the ω and the hcp phases; the latter two are very close to each other. Finally, in figure 5 we show for hcp Zr the pressure dependence of the 'constrained' bulk modulus $B_{(c/a)}$, of the unconstrained bulk modulus B and of the ratio k_c/k_a of the linear compressibilities along c and a.

4. Discussion

An apparent contradiction with experiment is the result that, at zero pressure, we find the lowest-energy phase to be not the hcp but the ω phase. This contradiction is only apparent because our calculations are valid at 0 K, whereas the experimental result applies to room temperature. The disagreement between theory and experiment may therefore by attributed to thermal effects. We note that the phase diagram of Zr calculated by Ostanin and Trubitsin [5] using the thermodynamic Gibbs function $G = E - TS + pV$ indeed has the ω phase as the ground state at zero pressure and zero temperature. We also note that a similar contradiction with experiment ($E_\omega < E_{\mathrm{hcp}}$) was found for Ti in [1–3], while in [3] the energy of the hcp structure of Zr was found to be only 0.25 mRyd/atom lower than that of the ω phase.

Since $G_\omega < G_{\mathrm{hcp}} < G_{\mathrm{bcc}}$ at 0 K in the pressure range below 50 kbar, we cannot discuss the hcp $\rightarrow \omega$ transition found experimentally at about 20 kbar, where we instead find a transition between the hcp and bcc phases. However, a real contradiction with experiment is found for the transition $\omega \rightarrow$ bcc, which we find to occur at about 50 kbar compared to the 300–350 kbar established by Ruoff and co-workers through diamond-anvil experiments [6, 7]. This discrepancy may be due partly to the calculations being valid only at 0 K and partly to the use of the LDA approximation. Thus, reference [3] finds the pressure for the $\omega \rightarrow$ bcc transition to be 112 kbar with LDA and 354 kbar with GGA, while [4] finds 178 kbar with LDA and 291 kbar with GGA, albeit in both cases by minimizing the energy, not the free energy.

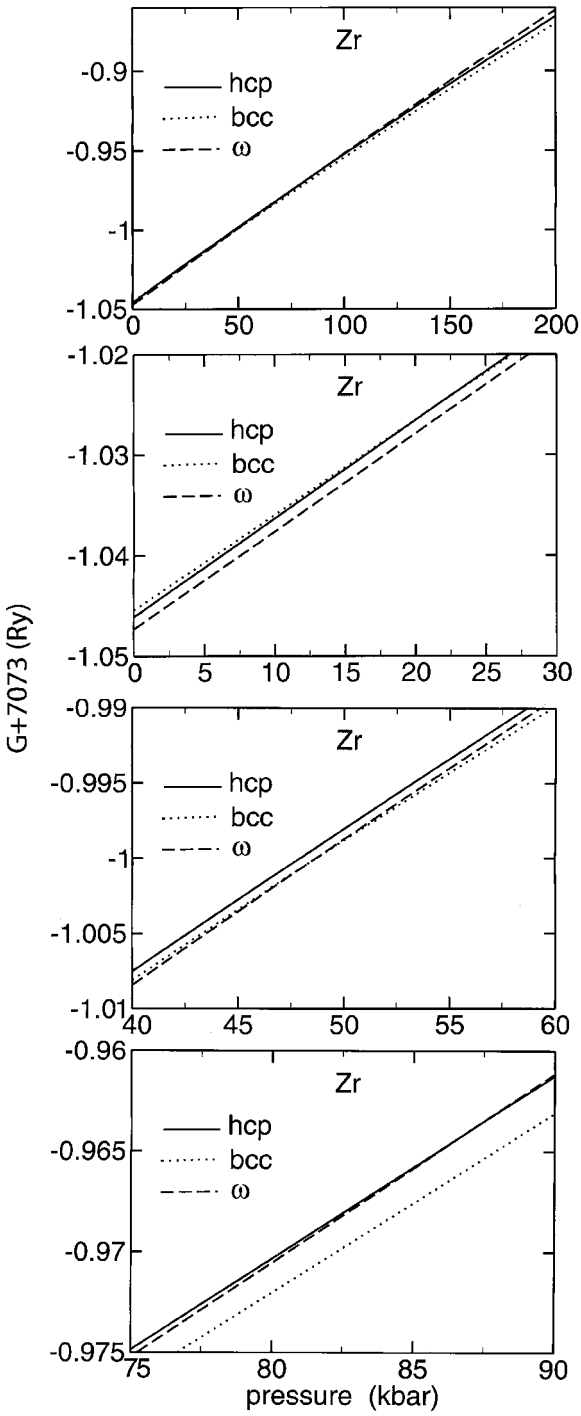

Figure 1. The pressure dependence of the free energy G for the hcp, bcc and ω phases of Zr. Top panel: the full range of pressures investigated in this work. Second panel: the pressure range 0 to 30 kbar, showing the crossing of the hcp and bcc free energies at about 20 kbar, while the ω free energy is lower than both. Third panel: the crossing of the bcc and ω free energies at about 50 kbar. Bottom panel: the hcp and ω free energies cross at about 87 kbar, while the bcc phase is lower than both.

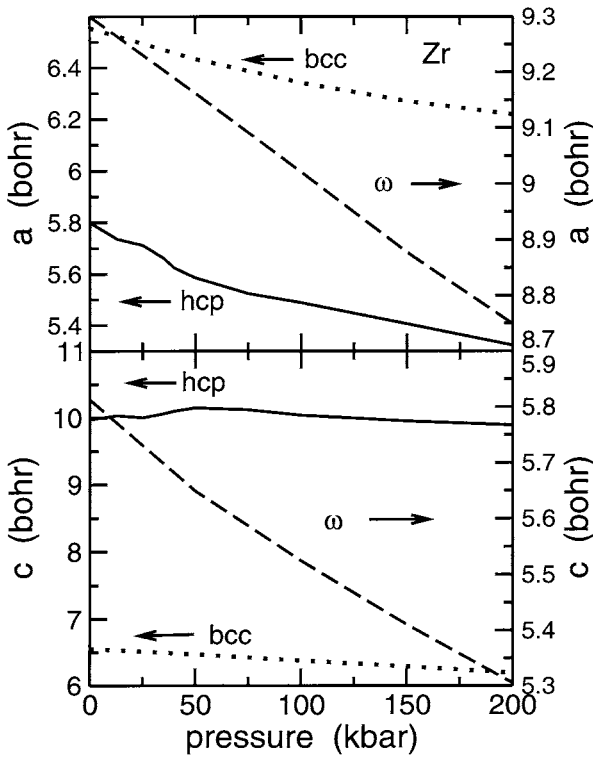

Figure 2. The pressure dependence of the lattice parameters a and c for the three Zr structures hcp, bcc and ω.

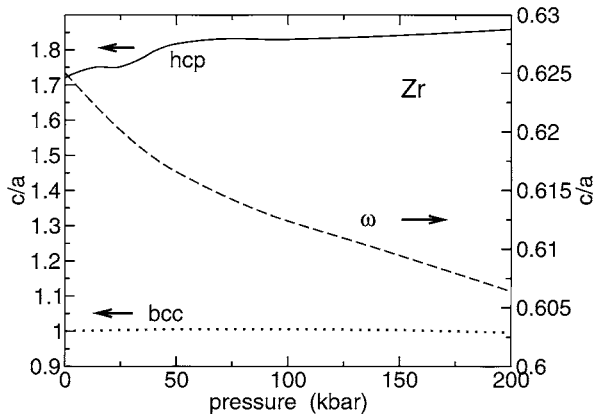

Figure 3. The changes in the axial ratio c/a of hcp, ω and bcc Zr with increasing hydrostatic pressure.

Figure 3 proves that the axial ratio c/a, which was assumed to be constant with varying volume in several published reports, does in fact exhibit a noticeable pressure dependence, While for the bcc structure the value of c/a remains practically unity up to 200 kbar, for the hcp structure it changes by about 6% between 0 and 50 kbar and for the ω structure it changes by about 3% in the same pressure range. These changes may have a significant effect on the energy curve as a function of volume and also on its derivative.

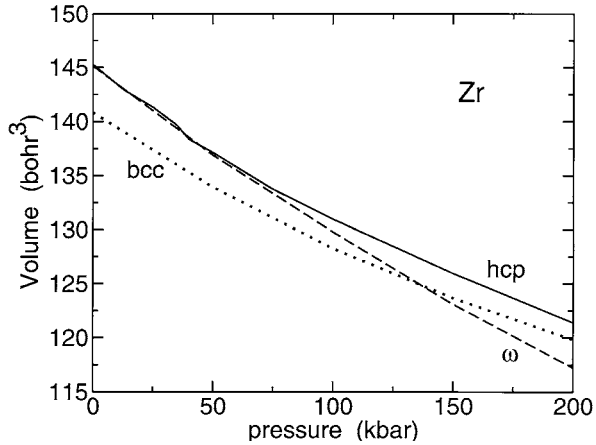

Figure 4. A plot of the equation of state for hcp, bcc and ω Zr.

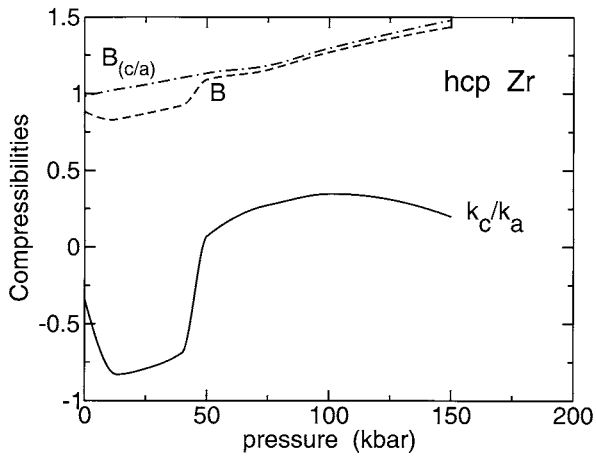

Figure 5. The bulk modulus B and the ratio of linear compressibilities k_c/k_a along the c- and the a-axes of hcp Zr exhibit marked anomalies in the pressure range 0–50 kbar, in contrast to the 'constrained' modulus $B_{(c/a)}$ (defined in the text).

The small anomalies shown by the lattice parameters and the axial ratio of hcp Zr in the range 0–50 kbar are magnified considerably by the elastic quantities that we plot in figure 5. An unexpected result is that the ratio of linear compressibilities k_c/k_a is negative in the pressure range from 0 to about 50 kbar. Both the bulk modulus B and k_c/k_a exhibit remarkable sensitivity to the phase changes occurring at 20 and 50 kbar. It is interesting to note that, by contrast, the bcc structure is wholly insensitive to either transition while the ω structure exhibits a change in slope at about 50 kbar. The 'constrained' bulk modulus $B_{(c/a)}$ of the hcp phase turns out to be largely insensitive to the transitions, showing directly that the c/a ratio can have a significant effect on the behaviour of material quantities in the vicinity of phase transitions.

Acknowledgments

We gratefully acknowledge partial support of this work by the National Science Foundation through Grant DMR0089274. P M Marcus thanks IBM for providing facilities as an Emeritus member of the Thomas J Watson Research Center.

References

[1] Gyanchandani J S, Gupta S C, Sikka S K and Chidambaram R 1990 *High Pressure Res.* **4** 472
[2] Ahuja R, Wills J M, Johansson B and Eriksson O 1993 *Phys. Rev.* B **48** 16269
[3] Jomard G, Magaud L and Pasturel A 1998 *Phil. Mag.* B **77** 67
[4] Grad G B, Blaha P, Luitz J, Schwarz K, Guillermet A F and Sferco S J 2000 *Phys. Rev.* B **62** 12743
[5] Ostanin S A and Trubitsin V Yu 1997 *Phys. Status Solidi* b **201** R9
[6] Hui Xia, Duclos S J, Ruoff A L and Vohra Y K 1990 *Phys. Rev. Lett.* **64** 204
[7] Hui Xia, Ruoff A L and Vohra Y K 1991 *Phys. Rev.* B **44** 10374
[8] Pearson W B 1967 *A Handbook of Lattice Spacings and Structures of Metals and Alloys* (Oxford: Pergamon)
[9] Kutsar A R 1975 *Fiz. Met. Metalloved.* **40** 786
Young D A 1991 *Phase Diagrams of the Elements* (Berkeley, CA: University of California Press)
Tonkov E Yu 1992 *High Pressure Phase Transformations—A Handbook* vol 2 (Philadelphia, PA: Gordon and Breach)
[10] An excellent description of the ω structure can be found at http://cst-www.nrl.navy.mil/lattice/struk/c32.html
[11] Jamieson J C 1963 *Science* **140** 72
[12] Vohra Y K 1978 *J. Nucl. Mater.* **75** 288
[13] Olinger B and Jamieson J C 1973 *High Temp.-High Pressure* **5** 123
[14] Sikka S K, Vohra Y K and Chidambaram R 1982 *Prog. Mater. Sci.* **27** 245
[15] Jona F and Marcus P M 2003 *Phys. Rev.* B submitted
[16] Blaha P, Schwarz K and Luitz J 1999 *WIEN97, A Full Potential Linearized Augmented Plane Wave Package for Calculating Crystal Properties* Technical University of Vienna (ISBN 3-9501031-0-4)
This is an improved and updated Unix version of the original copyrighted WIEN code, which was published by Blaha P, Schwarz K, Sorantin P and Trickey S B 1990 *Comput. Phys. Commun.* **59** 399
[17] Jona F and Marcus P M 2003 *J. Phys.: Condens. Matter* submitted
[18] Qiu S L and Marcus P M 2003 *Phys. Rev.* B at press
[19] Fast L, Ahuja R, Nordström L, Wills J M, Johansson B and Eriksson O 1997 *Phys. Rev. Lett.* **79** 2301